A novel PI3K/AKT Signaling Pathway-Associated Prognostic Signature Correlated With Immune Infiltration in Hepatocellular Carcinoma

Zhihuai Wang
  Dalian Medical University

Chen Xiong
  Dalian Medical University

Shuai Chen
  Dalian Medical University

Li Sun
  The Affiliated Changzhou No.2 People's Hospital of Nanjing Medical University

Peng Gao
  Dalian Medical University

Yuan Gao
  The Affiliated Changzhou No.2 People's Hospital of Nanjing Medical University

Chunfu Zhu
  The Affiliated Changzhou No.2 People's Hospital of Nanjing Medical University

Xihu Qin (✉ zcfmlm@njmu.edu.cn)
  The Affiliated Changzhou No.2 People's Hospital of Nanjing Medical University   https://orcid.org/0000-0002-0256-3478

Research Article

Abstract

Hepatocellular carcinoma (HCC) has become the third leading cause of death from cancer worldwide, and PI3K/AKT signaling pathway acts as the most common oncogenic pathway in HCC. But few studies have reported the prognostic value of PI3K/AKT associated genes (PAGs) and their association with immune infiltration. Hence, we downloaded the mRNA sequencing data and clinical information from The Cancer Genome Atlas (TCGA), GSE14520 dataset of Gene Expression Omnibus (GEO) and International Cancer Genome Consortium (ICGC) database. The 105 PAGs gene sets were from the Gene set enrichment analysis (GSEA) website. The biological processes of differently expressed PAGs were explored by Gene Ontology (GO) and Kyoto Encyclopedia of Genes and Genomes (KEGG) enrichment analysis. Then 4 prognostic PAGs (SFN, PRKAA2, PITX2 and CDK1) were identified through univariate and multivariate analyses. A prognostic signature was built base on the four PAGs. Afterward, the high-risk group had shorter survival time in Kaplan-Meier (KM) curves. Receiver operating characteristic (ROC) curves showed a better prognostic value of risk score (ROC=0.736) compared with other clinicopathological characteristics (AUC $\leq$ 0.511). The consistent results were obtained in the testing groups involving the GSE14520 dataset and ICGC database. The nomogram predicted the 1-year, 3-year, and 5-year overall survival rates in HCC. The correlation among risk score and immune infiltration of monocytes and M0 macrophages were determined, the expression levels of immune checkpoints (PDCD1, CTLA4, TIM3 and TIGIT) were also related to risk score in HCC. The study provided novel insight into the new targets for immunotherapy in HCC.

Introduction

Hepatocellular carcinoma (HCC) has become the rank-third malignant related to cancer deaths all over the world[1]. During the early stage, it is hard to obtain a clear HCC diagnosis, and effective treatments are not reliable to the majority of the patients. Some research has pointed out the great recurrence risk outcomes in the poor prognosis in patients with HCC[2]. Hence, searching for effective biomarkers for prognosis prediction as well as target spots for the patients' treatment utilizing HCC is essential.

Phosphatidylinositol 3-kinases (PI3Ks)/protein kinase B (AKT) signaling pathway was significant intracellular signaling react to extracellular stimulators, and it provided the novel insight into the new strategy for cancer therapy[3]. Recently some research had highlighted that the components of the PI3K/AKT signaling pathway were altered in different human tumors[4]. In particular, the PI3K/AKT/mTOR signaling pathway was often activated in the development and progression of HCC[5]. NCAPG can promote the proliferation of HCC through PI3K/AKT/FOXO4 pathway[6]. THBS4 also functioned as an oncogene in order to regulate the FAK/PI3K/AKT pathway during the development of HCC[7]. APLN participated in the PI3K/Akt pathway promoted the progression of HCC[8]. Interleukin-8 (IL-8) induced the invasion of HCC cells by participating in PI3K/Akt pathway[9]. Some research reported that apatinib can even enhance the sensitivity of radiotherapy by affecting the PI3K/AKT pathway[10]. It was also reported that VersicanV1 activated the EGFR−PI3K−AKT pathway to accelerate the proliferation and

metastasis of HCC[11]. However, the prognostic value of PI3K/AKT signaling pathway associated genes had not been elucidated yet.

Recent research had suggested that tumor-infiltrating lymphocytes (TILs) can inhibit tumor growth through protective immunity[12]. In some human cancers, particularly the levels of TILs were related to the patient's survival time[13–15]. The immune checkpoints (PD-1/PD-L1) blockade can reverse the exhausted CD8 + T cells through PI3K/Akt/mTOR pathway in gastrointestinal stromal tumors[16]. It was also reported that in breast cancer, the alteration of the PI3K/AKT signaling pathway was associated with the components of the tumor microenvironment, specifically, the infiltration of CD8 + lymphocytes had a significant correlation with the mutation of the PI3K/AKT signaling pathway[17]. However, the relationship between the levels of infiltrating lymphocytes and PI3K/AKT signaling pathway mutations in HCC was rarely reported.

In our study, the mRNA sequencing data and corresponding clinical information were acquired from The Cancer Genome Atlas (TCGA), Gene Expression Omnibus (GEO) and International Cancer Genome Consortium (ICGC) database. The PI3K/AKT signaling pathway associated genes (PAGs) were obtained from Gene set enrichment analysis (GSEA) online website. Then a prognostic signature was constructed on the basis of the 4 PAGs. The prognostic value of constructed prognostic signature was verified in three independent databases involving TCGA database, GEO database (GSE14520 dataset) and ICGC database. The association among the prognostic signature and the infiltrating immune cells and common immune checkpoints expression were investigated utilizing using CIBERSOFT and ESTIMATE algorithm. We concluded that the tumor immune microenvironment in HCC can be reflected by the constructed prognostic signature. The four-gene prognostic signature provided novel insight in predicting the therapeutic efficiency of immune checkpoints blockade in the immunotherapy of HCC, and it may provide new immunotherapeutic targets in HCC.

Materials And Methods

Data collection and analysis

The RNA sequencing data and corresponding clinical information were gathered from the TCGA website (https://portal.gdc.cancer.gov/), ICGC database (https://dcc.icgc.org/) and GEO database (GSE14520 dataset) (https://www.ncbi.nlm.nih.gov/geo/). The 105 PAGs were acquired from the HALLMARK_PI3K_AKT_MTOR_SIGNALING gene set of GSEA[18], whose website is http://www.broadinstitute.org/gsea/index.jsp.

The differentially expressed PAGs

The "limma" package was utilized to extract the differentially expressed PAGs by assessing the mRNA sequencing data of 105 PAGs in R software 4.0.2 (version 4.0.2, https://www.r-project.org/). Cut-off criteria set as |log2FC| >2, and $p < 0.05$ was significantly. The results were visualized through the volcano,

the heatmap and the boxplot. The employed R-packages included the "BiocManager", the "ggpubr" and the "pheatmap".

Function enrichment analysis of differently expressed PAGs

The underlying biological processes and signaling pathways correlated with differently expressed PAGs were analyzed by the Gene Ontology enrichment analysis (GO) and Kyoto Encyclopedia of Genes and Genomes (KEGG) pathway analysis. The results were eventually visualized by bar plots and the bubbles by using R 4.0.2 software. The employed R-packages involved the "ggpolt2", the "Cluster Profiler", the "enrich plot" and the "DOSE".

Constructing the PPI network

The STRING website (STRING: http://www.string-db.org/) was utilized to carry out the Protein-Protein interaction (PPI) network. The PPI network revealed the underlying interactions between the encoded proteins of differently expresses PAGs. It was eventually visualized by Cytoscape software, whose website is https://cytoscape.org/.

The establishment of four-gene prognostic signature

The univariate and multivariate Cox regression analyses were employed to identify the differently expressed PAGs with prognostic value. The prognostic signature was built in accordance with the multivariate Cox regression analysis results. The formula was illustrated as follows, Risk score = the expression level of gene 1×G1 + the expression level of gene 2×G2+...+the expression level of gene n×Gn (Gn refers to regression coefficient of prognostic gene in multivariate cox regression analysis). The four-gene prognostic signature formed by PAGs was carried out by using the "glmnet" package in R 4.0.2 software. Kaplan-Meier (K-M) curve and receiver operating characteristic (ROC) curve were employed to assess the predictive prognostic value of the constructed prognostic signature. The R-package ("rms") was utilized to plot the nomogram for predicting the survival rate of HCC patients.

ONCOMINE database

The ONCOMINE database (https://www.oncomine.org/resource/login.html)[19] performs the tumor-related analyses as an online website. The differential mRNA expression of 4 PAGs (SFN, PRKAA2, PITX2 and CDK1) were analyzed in 44 types of human cancers. The threshold parameters set as follows: p = 0.0001, fold change = 2, and gene rank of the top 10% genes. The p value was calculated utilizing the Student's t-test.

CBioPortal analysis

Cancer Genomics related cBioPortal (https://www.cbioportal.org/)[20] had been an online site capable of identifying, analyzing, and visualizing several human cancer's genomics data through a multidimensional perspective. The changes of genomic profiles involving the putative copy number alterations (CNAs), mutations, deep deletion as well as amplification were all analyzed by the website. The genetic

alterations of differently expressed prognostic PAGs (SFN, PRKAA2, PITX2 and CDK1) were calculated by the cBioPortal website.

Human Protein Atlas online website

The Human Protein Atlas online website (https://www.proteinatlas.org/)[21] was a human protein program that originated from Swedish. It was an online platform for analyzing multiple human proteins at the aspect of cells, tissues and organs by utilizing proteomics technology. The proteomics technology was comprised of systems biology, transcriptomics, antibody-based imaging and mass spectrometry-based proteomics. But the HPA database does not include protein expression data of PITX2. Fortunately, the expression of SFN, PRKAA2 and CDK1 at the protein levels were obtained from the Human Protein Atlas online website.

Statistical analysis

The Wilcoxon signed-rank test was used to analyze the differentially expressed genes between the HCC tumor tissues and normal tissues. The mRNA sequencing data were standardized through log2 transformation. The mRNA sequencing data and clinical information were both extracted by utilizing R 4.0.2 software (https://www.r-project.org/), and the Perl languages (https://www.perl.org/) was meanwhile employed to participate in the process. The abundance of immune cells infiltration in each sample was assessed through CIBERSORT method[22], the R packages involved "parallel", "e1071" and "BiocManager". The association between the immune infiltrating cells and risk score was examined through several packages ("vioplot", "BiocManager", "ggplot2", "ggpubr", "ggExtra", "scales", "ggtext" and "limma") in R software 4.0.2.

Results

Acquiring the differently expressed PAGs

The TCGA online website was employed to download the mRNA sequencing data and corresponding clinical information regarding 374 HCC tissue samples and 50 normal tissue samples. The clinicopathological information included age, gender, grade, TNM stage, T stage, N stage and M stage. The 105 PAGs were obtained from the HALLMARK_PI3K_AKT_MTOR_SIGNALING gene set of GSEA (Table S1). The 105 genes had been proved to associated with the PI3K/AKT/MTOR signaling pathway. The R 4.0.2 software "limma" package and the Wilcoxon signed-rank test method were employed to identify the differently expressed PAGs between tumor tissues and normal tissues in HCC (FDR < 0.05, |log FC| > 2). The results showed 9 upregulated PAGs were identified and it was presented by volcano plot (Fig. 1a). The boxplot (Fig. 1c) and heatmap (Fig. 1b) were also used to prove the differential mRNA expression of the above 9 upregulated genes.

GO and KEGG function enrichment analyses

Through GO and KEGG analyses, the biological processes and underlying pathways associated with 9 upregulated genes were identified. The top two significant biological processes included the regulation of G1/S transition of mitotic cell cycle and the regulation of cell cycle G1/S phase transition (Fig. 2a). The top two significant signaling pathways were Rap1 signaling pathway and calcium signaling pathway (Fig. 2b).

The establishment of PPI network

The correlation among the encoded proteins was analyzed by through STRING website and the results were visualized by Cytoscape software. The detail information of PPI network was also described by Cytoscape software (Fig. 2c). We identified the proteins whose degree of protein interaction was more than 30 by Cytoscape software, 10 hub genes were selected on the basis of the degree of protein interaction in PPI network, which included HRAS, MAPK8, PTEN, NGF, GRB2, RAC1, EGFR, MAPK1, AKT1 and GSK3B (Fig. 2d).

Searching for the hub PAGs associated with prognosis

The univariate cox regression analysis and multivariate cox regression analysis were employed to identify the differently expressed PAGs with prognostic value. The univariate Cox regression analysis obtained six prognostic PAGs including PLCB1, SFN, PRKAA2, PITX2, CDK1 and E2F1 (Fig. 3a). The final four prognostic PAGs (SFN, PRKAA2, PITX2, CDK1) for constructing the prognostic signature were screened out through multivariate cox regression analysis (Fig. 3b). The regression coefficients were exhibited in Table 1.

Table 1
Multivariate Cox regression results of prognosis-related PAGs in HCC

Gene id	Coefficient	HR	HR.95L	HR.95H	P value
SFN	0.116124	1.123135	1.029512	1.225273	0.008925
PRKAA2	0.204509	1.226922	1.011449	1.488299	0.037941
PITX2	0.443949	1.558850	1.049609	2.315162	0.027815
CDK1	0.222894	1.249688	1.043175	1.497084	0.015579

Note: PAGs: the phosphoinositide 3-kinase (PI3K)/protein kinase B (AKT) associated genes; HCC, hepatocellular carcinoma; HR, hazard ratio.

Constructing the PAGs-associated prognostic signature

In accordance with the four selected PAGs (SFN, PRKAA2, PITX2, CDK1) and their regression coefficients, the prognostic signature was constructed and the formula utilized was PAGs-associated prognostic signature = (0.443949 * the expression level of PITX2) + (0.204509 * the expression level of PRKAA2) + (0.222894 * the expression level of CDK1) + (0.116124 * the expression level of SFN). The risk score of patients were calculated by the formula. The four-gene prognostic signature split patients into the high-

risk cohort and the low-risk cohort on the basis of risk sscore (Fig. 3d). The significant differential expression of PITX2, PRKAA2, CDK1 and SFN were identified between the high-risk cohort and the low-risk cohort, and it was visualized by heatmap (Fig. 3c). The survival time of HCC patients was considerably reduced along with the increasing risk score in the scatterplot, and the proportion of dead samples meanwhile increased (Fig. 3e). The KM curve showed that the survival probability of HCC patients was poorer in the high-risk cohort compared with low-risk cohort (p = 4.817 E-05; Fig. 4a). The samples of the high-risk cohort and the low-risk cohort were up to 185.

The get set enrichment analysis of the prognostic signature

The underlying mechanism correlated with the prognostic signature was analyzed in KEGG enrichment analysis. The results revealed that the risk score was associated with 5 upregulated biological signaling pathway and 2 downregulated biological signaling pathway. The upregulated signaling pathway involved the cell cycle, the insulin signaling pathway, the MTOR signaling pathway, the NOTCH signaling pathway and the p53 signaling pathway. While the downregulated signaling pathway included the fatty acid metabolism signaling pathway and PPAR signaling pathway (Fig. 4b).

Comparing the independent prognostic value of the prognostic signature with clinicopathological characteristics

The ROC curve was performed to compare the independent prognostic value between the constructed prognostic signature and various clinicopathological characteristic. The results showed prognostic value of constructed signature (AUC = 0.736) was greater than other clinicopathological characteristics (AUC $\leq$ 0.511) (Fig. 4c). The ROC curve evaluated the accuracy of prognostic signature and the area below the ROC curve were all statistically significant (1-year AUC, 0.737; 2-year AUC, 0.704; 3-year AUC, 0.694; Fig. 4d). The univariate and multivariate cox regression analyses were carried out to investigate the independent prognostic value of the constructed signature adjusted by several clinicopathological characteristics. The clinicopathologic characteristics were consist of age, gender, grade, T stage, M stage and N stage. All results suggested that the risk score of the prognostic signature had potential to be the independent prognostic factor in hepatocellular carcinoma (hazard ratio > 1; p < 0.001; Fig. 4e-f).

The differential expression of 4 PAGs and their prognostic value in HCC

The mRNA expression of SFN, CDK1, PRKAA2 and PITX2 were all elevated in HCC tissue samples compared with normal tissue samples (Figure S1a). The consistent results were gained in ONCOMINE database (Figure S2a), but the expression data of PITX2 wasn't involved in ONCOMINE database. The four elevated PAGs expression were all correlated with the poor survival of HCC patients (Figure S1b). We further employed cBioPortal online website to determine the genetic alternations of four PAGs in HCC. The results showed that the deep deletion, the amplification, the truncating mutation and the missense

mutation were all observed among the changes, and the deep deletion was the most common (Figure S2c). The human protein atlas (HPA) database was also utilized to verify the elevated expression of the four PAGs at the protein levels (Figure S2b). The expression data of PITX2 wasn't involved in HPA. We explored the expression of 3 PAGs (SFN, CDK1 and PRKAA2) at the protein levels in this website. The results highlighted that SFN, CDK1 and PRKAA2 were all elevated in tumor tissues compared with the normal tissues.

Relationship between the prognostic risk model and clinicopathological characteristics

The relationship among the prognostic signature and clinicopathological characteristics was further investigated. The data composed of mRNA sequencing data and corresponding clinical information was originated from TCGA database. The results showed that the risk score was associated with the stage (p = 7.9E-05; Figure S3a), the grade (p = 1.8E-07; Figure S3b) and the T classification (p = 0.00015; Figure S3c), the expression of CDK1 was also related to the stage (p = 0.0034; Figure S3d), the grade (p = 4.5E-08; Figure S3e) and the T classification (p = 0.004; Figure S3f), the PRKAA2 expression was associated with the stage (p = 0.022; Figure S3g), the grade (p = 0.00035; Figure S3h) and the T classification (p = 0.049; Figure S3i). The PITX2 expression was related with stage (p = 0.00011; Figure S3j) and T classification (p = 0.00094; Figure S3k). The expression of SFN was associated with the grade (p = 0.032; Figure S3l).

To validate the prognostic value of constructed prognostic signature in GSE14520 dataset and ICGC database

To validate the potent prognostic value of constructed prognostic signature and verify its accuracy, we further downloaded the ICGC data and GSE14520 dataset. In the testing group of GSE14520 dataset. The HCC patients were divided into the high-risk cohort and low-risk cohort based on the value of risk score (Fig. 5c). The survival time of patients was significantly reduced accompanied by the increasing risk score of patients in the scatterplot (Fig. 5e), The significant differential expression of PITX2, PRKAA2, CDK1 and SFN were identified and visualized by heatmap (Fig. 5a). The KM curves indicated that high risk score was correlated with the poor prognosis of HCC patients (p = 1.812E-04; Fig. 5g). To further identify the prognostic value of constructed prognostic signature. We likewise used the data originated from ICGC database to verify it. The HCC patients were also categorized into the high-risk cohort and low-risk cohort based on the value of risk score (Fig. 5d). The results showed the high-risk group has shorter survival time than the low-risk group (Fig. 5f), The significant differential expression of 4 PAGs (SFN, PRKAA2, PITX2 and CDK1) in ICGC database (Fig. 5b) were also identified and visualized by heatmap. In the KM curve, the high-risk group had a lower survival probability in comparison to the low-risk group (p = 6.493E-05; Fig. 5h). The ROC curve was constructed to assess the accuracy of prognostic signature by analyzing the data from both GSE14520 dataset (Fig. 5i) and ICGC database (Fig. 5j). The area below the ROC curve had a better predictive significance in both GSE14520 dataset and ICGC database (1-year AUC, 0.632 vs 0.784; 2-year AUC, 0.646 vs 0.727; 3-year AUC, 0.650 vs 0.758).

The nomogram was constructed for predicting prognosis

The nomogram was constructed on the basis of the different clinicopathology characteristics and risk scores. The clinical prognostic value of conducted prognostic signature was developed by the nomogram. The 1-year survival, 2-year survival, and 3-year survival of HCC patients were predicted by the total point (Fig. 6a). The calibration plots revealed good coherence between the realistic outcome and the prediction of nomogram (Fig. 6c-d).

The risk score was associated the immune infiltration in HCC

The concrete composition of infiltrating immune cells was calculated by utilizing CIBERSORT method, the results suggested the percentage of infiltrating immune cells in each TCGA sample (Fig. 7a). The different infiltrating immune cells had a slight correlation with each other (Fig. 7b). The samples were divided into two groups based on the median value of risk score. We also employed a heatmap to determine the difference between the high-risk group and the low-risk group (Fig. 8a). The results demonstrated that the infiltrating M0 macrophages and Monocytes were differently enriched between the two groups, and the infiltrating levels of Monocytes was higher in low-risk group. The infiltrating levels of M0 macrophages was greater in high-risk group compared with the low-risk group (Fig. 8b). It is worth mentioning that the risk score was positively correlated with B cells, CD4 + T cells, neutrophil, macrophages and Myeloid dendritic cells in TIMER database (Figure S2a). Particularly the macrophages M0 and neutrophils were strongly associated with the risk score (Figure S2b and S2c).

The risk score was correlated with the expression levels of immune checkpoints

Recent studies indicated the application of immune checkpoints inhibitors was not efficient in HCC patients[23]. Hence, we investigated the association between the prognostic signature and the several immune checkpoints (PD-1, PD-L1, PD-L2, CTLA4, TIM3, LAG3, TIGIT, CD96). The results showed the risk score was correlated with the expression levels of PD-1, CTLA4, TIM3, and TIGIT, and the expression of above immune checkpoints was higher in high- risk group compared with low-risk group (Fig. 8c). It indicated that the risk score can reflect the expression levels of immune checkpoints and it had great predictive value for the sensitivity of immune checkpoints inhibitors in HCC.

Discussion

Although the diagnosis, prognosis prediction, and treatment strategies of HCC have made great progress, hepatocellular carcinoma remained to be the major cause of cancer death worldwide[23–25]. At the same time, the PI3K/AKT/mTOR signaling pathway acted as a key cellular signaling pathway associated with the appearance of several human cancers[26]. The inhibitors of the PI3K/AKT/mTOR signaling pathway

were thoroughly studied and evaluated in clinical trials in human cancers[27]. It had been suggested that PI3K/AKT signaling pathway associated genes can serve as the potential biomarkers for the development of numerous human cancer[28]. However, few studies mentioned the prognostic value of PAGs in HCC. Some research indicated constructing the early predictive model for prognosis in human cancer is necessary[29], and the different therapeutic strategy should be formulated according to different prognosis of patients[30, 31]. Currently, an opinion had been recommended that clinicopathological characteristics can be employed to predict prognosis of patients, but some studies highlighted that clinicopathological characteristics can't provide adequate evidence for accurate prognostic evaluation[32, 33]. Thus, we constructed a novel prognostic signature based on the PI3K/AKT signaling pathway associated genes in HCC. Recent studies have shown that the immune escape and tolerance can be mediated through various signaling pathways in tumor microenvironment[34]. Hence, the association between constructed prognostic signature and immune infiltration was also determined.

In this study, we developed a prognostic signature consisted of 4 PAGs based on TCGA database. The prognostic value and accuracy of constructed prognostic signature were further validated in GSE14520 dataset and ICGC database. First of all, the mRNA sequencing data and corresponding clinical information were downloaded from the TCGA database, and 105 PAGs were obtained from GSEA online website. Subsequently, 9 upregulated PAGs were screened out from 374 HCC tissue samples and 50 normal tissue samples. The GO and KEGG enrichment analysis were further employed to investigate the biological processes correlated with the upregulated PAGs. The PPI network was utilized to exhibit the connection between encoded proteins, and the hub genes (HRAS, MAPK8, PTEN, NGF, GRB2, RAC1, EGFR, MAPK1, AKT1 and GSK3B) were screened out in the PPI network. The univariate and multivariate Cox regression analyses were employed to identify the differently expressed genes associated with the prognosis of patients. We developed the prognostic signature based on the 4 PAGs. The independent prognostic value of 4-gene-signature was identified by univariate and multivariate regression analyses. The KM curve showed the low-risk cohort had the higher survival probability in comparison to the high-risk cohort. The area under the ROC curve indicated the 4-gene-signature had a larger prognostic value compared with other clinicopathologic characteristics. The consistent results were obtained in the GSE14520 dataset and ICGC database. Ultimately the nomogram was created to accurately predict the 1-year, 3-year, and 5-year overall survival rates in HCC. The risk score was correlated with the infiltration of monocytes and macrophages M0 in HCC, and the expression levels of common immune checkpoints (PDCD1, CTLA4, TIM3 and TIGIT) was associated with the risk score.

It was proved that immunosuppressive microenvironment enhanced the evasion and immune tolerance in HCC[34]. HCC is a type of malignant tumor accompanied by chronic liver inflammation and liver cirrhosis, some HCC cases expressed gene markers indicating the immune response, which provided a novel insight into immune therapy for HCC[35]. Our results showed the infiltrating levels of monocyte and Macrophages M0 were higher in high-risk group, which was consistent with the poorer survival in HCC. Tumor associated macrophages (TAMs) are essential elements in HCC microenvironment and lead to the poor survival in HCC patients[36]. TAMs obtained the immunosuppressive function to regulate the tumor microenvironment as they grow from monocytes to macrophages[37]. Current studies even reported that

macrophages were the most common immune cells in tumor tissues and it induced the invasion, proliferation and metastasis in tumor cells, it also mediated the immune tolerance in tumor microenvironment[38–40]. We further calculated the correlation between the risk score and several common immune checkpoints including PDCD1(PD-1), PDL1, PDL2, CTLA4, TIM3, LAG3, TIGIT and CD96. And the results showed the expression levels of PDCD1, CTLA4, TIM3 and TIGIT were associated with risk score. Some research indicated that anti-PD-1 and anti-CTLA4 antibodies tended to be the effective clinical therapeutic targets in HCC[41], and PD-1 inhibitor (nivolumab) can stimulate the specific immune response with controllable side effects in tumor[42]. However, the response to immune checkpoints in HCC was different among various organs[43]. Our results hinted that our risk score can revealed the expression of immune checkpoints and explained why the efficacy of anti-immune checkpoints was low in some HCC patients. The four-gene-signature had potential to predict the therapeutic efficacy of PD-1, CTLA4, TIM3 and TIGIT, and provided the guidance for therapeutic strategy in immunotherapy.

Previous research had pointed out the crucial role of PRKAA2 in human cancers. PRKAA2 functioned as a member of heterotrimeric AMP-activated protein kinase (AMPK) complex, and was reported to be involved in the p53 and mTOR signaling pathways in carcinogenesis of human cancers[44]. In our study, PRKAA2 was identified as the PAG and determined its prognostic value. Current studies indicated that MiR-4999-5p can promote the cell growth and glycolysis by targeting PRKAA2 in colorectal cancer[45], and PRKAA2 was also dysregulated in cervical cancer cells and had potential to be the prognostic biomarker in cervical cancer[46]. Some research had likewise suggested that metformin suppressed the proliferation of HCC cells by targeting miR-378/CDK1 axis[47]. The inhibition of CDK1/PDK1/β-Catenin pathway can improve the therapeutic effect of sorafenib and suppress the proliferation of HCC cells[48]. SNHG16 activated the let-7b-5p/CDC25B/CDK1 axis to influence the G2/M transition resulting in the accelerating progression of EMT and cell metastasis[49]. Circular RNA (circ-ADD3) suppressed the metastasis of HCC cells through the ubiquitination mediated by CDK1[50]. We therefore can summarize that CDK1 was an important regulatory factor in the carcinogenesis of HCC. PITX2 also plays a carcinogenic role in several human cancers. The overexpression of PITX2 can induce the letrozole-resistance in breast cancer cells[51], and it also participated in the progression of ovarian cancer by promoting the proliferation and invasion of ovarian cancer cells[52]. The methylation of PITX2 also served as a prognostic biomarker in colorectal cancer[53], and it was reported to mediate proliferation and invasion of colorectal cancer cells in vitro experiment[54]. In human gliomas, SFN was reported to be the potential prognostic biomarker[55], and it provided great prognostic value in the progression of esophageal squamous cell carcinoma[56]. The overexpression of SFN was correlated with the poor prognosis in ovarian cancer and pancreatic ductal adenocarcinoma[57, 58].

Conclusions

To determine the prognostic value of PAGs and their association with immune infiltration in HCC, we established a four-gene prognostic signature associated with PI3K/AKT signaling pathway. A strong relationship among the risk score, immune infiltrating cells and immune checkpoints was also identified.

In order to predict the prognosis of HCC patients, a nomogram was established based on the risk score. The great prognostic value of the four-gene prognostic signature was trained in TCGA database, and it was further tested in both GSE14520 dataset and ICGC database. It was concluded that the four-gene-signature had better prognostic value in comparison to other clinicopathological characteristics. This is the first study to discuss the prognostic value of PI3K/AKT associated genes and their association with immune infiltration in HCC. Our study offered a novel insights into new biomarkers and the guidance for therapeutic strategy in immunotherapy of HCC, and we identified the association between PI3K/AKT signaling pathway alterations and immune microenvironment in HCC.

Abbreviations

HCC: hepatocellular carcinoma; TCGA: The Cancer Genome Atlas; ICGC: International Cancer Genome Consortium; GEO: Gene Expression Omnibus; PAGs: PI3K/AKT signaling pathway-associated genes; GSEA: gene set enrichment analysis; GO: Gene Ontology; KEGG: Kyoto Encyclopedia of Genes and Genomes; PPI: protein-protein interaction; CNAs: copy number alterations; HPA: human protein atlas; ROC: receiver operating characteristic; K-M: Kaplan-Meier; AUC: the area under the ROC curve; TNM: Tumor size/lymph nodes/distance metastasis.

Declarations

Funding

Conflicts of interest

The authors declare that they have no competing interests.

Availability of data and materials

The datasets analyzed were acquired from The Cancer Genome Atlas (TCGA) database (https://portal.gdc.cancer.gov/), International Cancer Genome Consortium (ICGC) database (https://dcc.icgc.org/) and Gene Expression Omnibus (GEO) database (https://www.ncbi.nlm.nih.gov/geo/).

Code availability

Not applicable.

Authors' contributions

ZHW and CX contributed to the conception and design of the study; ZHW and SC collected data and wrote the manuscript; ZHW performed the data analysis and constructed the figures and tables; ZHW, CX, SC, LS, PG, YG, CFZ and XHQ reviewed and revised the manuscript and were involved in the conception of the study. Additionally, XHQ was responsible for the organization, revision and submission of this manuscript. All authors read and approved the final manuscript.

Ethics approval

Not applicable.

Consent to participate

Not applicable.

Consent for publication

All the authors consented to the publication of this research.

Acknowledgments

References

1. Sung H, Ferlay J, Siegel RL et al (2021) Global cancer statistics 2020: GLOBOCAN estimates of incidence and mortality worldwide for 36 cancers in 185 countries. CA CANCER J CLIN 0:41

2. Gu Y, Li X, Bi Y et al (2020) CCL14 is a prognostic biomarker and correlates with immune infiltrates in hepatocellular carcinoma. aging 12:784–807. https://doi.org/10.18632/aging.102656

3. Noorolyai S, Shajari N, Baghbani E et al (2019) The relation between PI3K/AKT signalling pathway and cancer. Gene 698:120–128. https://doi.org/10.1016/j.gene.2019.02.076

4. Vara JÁF, Casado E, de Castro J et al (2004) PI3K/Akt signalling pathway and cancer. Cancer Treat Rev 30:193–204. https://doi.org/10.1016/j.ctrv.2003.07.007

5. Dimri M, Satyanarayana A (2020) Molecular Signaling Pathways and Therapeutic Targets in Hepatocellular Carcinoma. Cancers 12:491. https://doi.org/10.3390/cancers12020491

6. Gong C, Ai J, Fan Y et al (2019) NCAPG Promotes The Proliferation Of Hepatocellular Carcinoma Through PI3K/AKT Signaling. OTT Volume 12:8537–8552. https://doi.org/10.2147/OTT.S217916

7. Guo D, Zhang D, Ren M et al (2020) THBS4 promotes HCC progression by regulating ITGB1 via FAK/PI3K/AKT pathway. FASEB j 34:10668–10681. https://doi.org/10.1096/fj.202000043R

8. Chen H, Wong C-C, Liu D et al (2019) APLN promotes hepatocellular carcinoma through activating PI3K/Akt pathway and is a druggable target. Theranostics 9:5246–5260.

https://doi.org/10.7150/thno.34713

9. Sun F, Wang J, Sun Q et al (2019) Interleukin-8 promotes integrin β3 upregulation and cell invasion through PI3K/Akt pathway in hepatocellular carcinoma. J Exp Clin Cancer Res 38:449. https://doi.org/10.1186/s13046-019-1455-x

10. Liao J, Jin H, Li S et al (2019) Apatinib potentiates irradiation effect via suppressing PI3K/AKT signaling pathway in hepatocellular carcinoma. J Exp Clin Cancer Res 38:454. https://doi.org/10.1186/s13046-019-1419-1

11. Zhangyuan G, Wang F, Zhang H et al (2020) VersicanV1 promotes proliferation and metastasis of hepatocellular carcinoma through the activation of EGFR−PI3K−AKT pathway. Oncogene 39:1213−1230. https://doi.org/10.1038/s41388-019-1052-7

12. Fridman WH, Pagès F, Sautès-Fridman C, Galon J (2012) The immune contexture in human tumours: impact on clinical outcome. Nat Rev Cancer 12:298−306. https://doi.org/10.1038/nrc3245

13. Vaziri Fard E, Ali Y, Wang XI et al (2019) Tumor-Infiltrating Lymphocyte Volume Is a Better Predictor of Disease-Free Survival Than Stromal Tumor-Infiltrating Lymphocytes in Invasive Breast Carcinoma. Am J Clin Pathol 152:656−665. https://doi.org/10.1093/ajcp/aqz088

14. Okada K, Komuta K, Hashimoto S et al Frequency of Apoptosis of Tumor-infiltrating Lymphocytes Induced by Fas Counterattack in Human Colorectal Carcinoma and Its Correlation with Prognosis. 6

15. Puccetti L, Manetti R, Parronchi P et al (2002) Role of low nuclear grading of renal carcinoma cells in the functional profile of tumor-infiltrating T cells. Int J Cancer 98:674−681. https://doi.org/10.1002/ijc.10238

16. Zhao R, Song Y, Wang Y et al (2019) PD-1/PD-L1 blockade rescue exhausted CD8 + T cells in gastrointestinal stromal tumours via the PI3K/Akt/mTOR signalling pathway. Cell Prolif 52:e12571. https://doi.org/10.1111/cpr.12571

17. Sobral-Leite M (2019) Cancer-immune interactions in ER-positive breast cancers: PI3K pathway alterations and tumor-infiltrating lymphocytes. 12

18. Subramanian A, Tamayo P, Mootha VK et al (2005) Gene set enrichment analysis: A knowledge-based approach for interpreting genome-wide expression profiles. Proceedings of the National Academy of Sciences 102:15545−15550. https://doi.org/10.1073/pnas.0506580102

19. Rhodes DR, Kalyana-Sundaram S, Mahavisno V et al (2007) Oncomine 3.0: Genes, Pathways, and Networks in a Collection of 18,000 Cancer Gene Expression Profiles. Neoplasia 9:166−180. https://doi.org/10.1593/neo.07112

20. Cerami E, Gao J, Dogrusoz U et al (2012) The cBio Cancer Genomics Portal: An Open Platform for Exploring Multidimensional Cancer Genomics Data: Fig. 1. Cancer Discov 2:401−404. https://doi.org/10.1158/2159-8290.CD-12-0095

21. Pontén F, Schwenk JM, Asplund A, Edqvist P-HD (2011) The Human Protein Atlas as a proteomic resource for biomarker discovery: Review: The Human Protein Atlas. J Intern Med 270:428−446. https://doi.org/10.1111/j.1365-2796.2011.02427.x

22. Newman AM, Liu CL, Green MR et al (2015) Robust enumeration of cell subsets from tissue expression profiles. Nat Methods 12:453–457. https://doi.org/10.1038/nmeth.3337

23. Rebouissou S (2020) Advances in molecular classification and precision oncology in hepatocellular carcinoma. J Hepatol 72:15

24. Banaudha KK, Verma M (2015) Epigenetic Biomarkers in Liver Cancer. In: Verma M (ed) Cancer Epigenetics. Springer New York, New York, pp 65–76

25. Liu G-M, Zeng H-D, Zhang C-Y, Xu J-W (2019) Identification of a six-gene signature predicting overall survival for hepatocellular carcinoma. Cancer Cell Int 19:138. https://doi.org/10.1186/s12935-019-0858-2

26. Alzahrani AS (2019) PI3K/Akt/mTOR inhibitors in cancer: At the bench and bedside. Semin Cancer Biol 59:125–132. https://doi.org/10.1016/j.semcancer.2019.07.009

27. Courtney KD, Corcoran RB, Engelman JA (2010) The PI3K Pathway As Drug Target in Human Cancer. JCO 28:1075–1083. https://doi.org/10.1200/JCO.2009.25.3641

28. Chen P, Shi P, Du G et al Wnt/β-Catenin, Carbohydrate Metabolism, and PI3K-Akt Signaling Pathway-Related Genes as Potential Cancer Predictors. Journal of Healthcare Engineering 8

29. Forner A, Reig M, Bruix J (2018) Hepatocellular carcinoma. The Lancet 391:1301–1314. https://doi.org/10.1016/S0140-6736(18)30010-2

30. Bejar R, Stevenson KE, Caughey BA et al (2012) Validation of a Prognostic Model and the Impact of Mutations in Patients With Lower-Risk Myelodysplastic Syndromes. JCO 30:3376–3382. https://doi.org/10.1200/JCO.2011.40.7379

31. Yamamoto N, Watanabe T, Katsumata N et al (1998) Construction and validation of a practical prognostic index for patients with metastatic breast cancer. JCO 16:2401–2408. https://doi.org/10.1200/JCO.1998.16.7.2401

32. Lee J-H, Jung S, Park WS et al (2019) Prognostic nomogram of hypoxia-related genes predicting overall survival of colorectal cancer–Analysis of TCGA database. Sci Rep 9:1803. https://doi.org/10.1038/s41598-018-38116-y

33. Wang X, Yao S, Xiao Z et al (2020) Development and validation of a survival model for lung adenocarcinoma based on autophagy-associated genes. J Transl Med 18:149. https://doi.org/10.1186/s12967-020-02321-z

34. Fu Y, Liu S, Zeng S, Shen H (2019) From bench to bed: the tumor immune microenvironment and current immunotherapeutic strategies for hepatocellular carcinoma. J Exp Clin Cancer Res 38:396. https://doi.org/10.1186/s13046-019-1396-4

35. Okusaka T, Ikeda M (2018) Immunotherapy for hepatocellular carcinoma: current status and future perspectives. ESMO Open 3:e000455. https://doi.org/10.1136/esmoopen-2018-000455

36. Lu C, Rong D, Zhang B et al (2019) Current perspectives on the immunosuppressive tumor microenvironment in hepatocellular carcinoma: challenges and opportunities. Mol Cancer 18:130. https://doi.org/10.1186/s12943-019-1047-6

37. Galdiero MR, Bonavita E, Barajon I et al (2013) Tumor associated macrophages and neutrophils in cancer. Immunobiology 218:1402–1410. https://doi.org/10.1016/j.imbio.2013.06.003

38. Mantovani A, Marchesi F, Malesci A et al (2017) Tumour-associated macrophages as treatment targets in oncology. Nat Rev Clin Oncol 14:399–416. https://doi.org/10.1038/nrclinonc.2016.217

39. Degroote H, Van Dierendonck A, Geerts A et al (2018) Preclinical and Clinical Therapeutic Strategies Affecting Tumor-Associated Macrophages in Hepatocellular Carcinoma. Journal of Immunology Research 2018:1–9. https://doi.org/10.1155/2018/7819520

40. Gajewski TF, Schreiber H, Fu Y-X (2013) Innate and adaptive immune cells in the tumor microenvironment. Nat Immunol 14:1014–1022. https://doi.org/10.1038/ni.2703

41. Wheeler DA (2018) Comprehensive and Integrative Genomic Characterization of Hepatocellular Carcinoma. 54

42. Hida T (2018) Nivolumab for the treatment of Japanese patients with advanced metastatic non-small cell lung cancer: a review of clinical trial evidence for efficacy and safety. Ther Adv Respir Dis 12:175346661880116. https://doi.org/10.1177/1753466618801167

43. Lu L-C, Hsu C, Shao Y-Y et al (2019) Differential Organ-Specific Tumor Response to Immune Checkpoint Inhibitors in Hepatocellular Carcinoma. Liver Cancer 8:480–490. https://doi.org/10.1159/000501275

44. Hoffman AE, Demanelis K, Fu A et al (2013) Association of AMP-Activated Protein Kinase with Risk and Progression of Non–Hodgkin Lymphoma. Cancer Epidemiol Biomarkers Prev 22:736–744. https://doi.org/10.1158/1055-9965.EPI-12-1014

45. Zhang Q, Hong Z, Zhu J et al (2020) miR-4999-5p Predicts Colorectal Cancer Survival Outcome and Reprograms Glucose Metabolism by Targeting PRKAA2. OTT Volume 13:1199–1210. https://doi.org/10.2147/OTT.S234666

46. Choi CH, Chung J-Y, Cho H et al (2015) Prognostic Significance of AMP-Dependent Kinase Alpha Expression in Cervical Cancer. Pathobiology 82:203–211. https://doi.org/10.1159/000434726

47. Zhou J, Han S, Qian W et al (2018) Metformin induces miR-378 to downregulate the CDK1, leading to suppression of cell proliferation in hepatocellular carcinoma. OTT Volume 11:4451–4459. https://doi.org/10.2147/OTT.S167614

48. Wu CX, Wang XQ, Chok SH et al (2018) Blocking CDK1/PDK1/β-Catenin signaling by CDK1 inhibitor RO3306 increased the efficacy of sorafenib treatment by targeting cancer stem cells in a preclinical model of hepatocellular carcinoma. Theranostics 8:3737–3750. https://doi.org/10.7150/thno.25487

49. Li S, Peng F, Ning Y et al (2020) SNHG16 as the miRNA let-7b-5p sponge facilitates the G2/M and epithelial-mesenchymal transition by regulating CDC25B and HMGA2 expression in hepatocellular carcinoma. J Cell Biochem 121:2543–2558. https://doi.org/10.1002/jcb.29477

50. Sun S, Wang W, Luo X et al Circular RNA circ-ADD3 inhibits hepatocellular carcinoma metastasis through facilitating EZH2 degradation via CDK1-mediated ubiquitination. 17

51. Xu Y, Yu H, Sun J et al (2019) Upregulation of PITX2 Promotes Letrozole Resistance Via Transcriptional Activation of IFITM1 Signaling in Breast Cancer Cells. Cancer Res Treat 51:576–592.

https://doi.org/10.4143/crt.2018.100

52. Fung FKC, Chan DW, Liu VWS et al (2012) Increased Expression of PITX2 Transcription Factor Contributes to Ovarian Cancer Progression. PLoS ONE 7:e37076. https://doi.org/10.1371/journal.pone.0037076

53. Semaan A Significance of PITX2 Promoter Methylation in Colorectal Carcinoma Prognosis. 9

54. Hirose H, Ishii H, Mimori K et al (2011) The Significance of PITX2 Overexpression in Human Colorectal Cancer. Ann Surg Oncol 18:3005–3012. https://doi.org/10.1245/s10434-011-1653-z

55. Deng J (2011) Stratifin expression is a novel prognostic factor in human gliomas. 6

56. Ren H-Z, Pan G, Wang J-S et al (2010) Reduced Stratifin Expression Can Serve As an Independent Prognostic Factor for Poor Survival in Patients with Esophageal Squamous Cell Carcinoma. Dig Dis Sci 55:2552–2560. https://doi.org/10.1007/s10620-009-1065-0

57. Hu Y, Zeng Q, Li C, Xie Y (2019) Expression profile and prognostic value of SFN in human ovarian cancer. Biosci Rep 39:BSR20190100. https://doi.org/10.1042/BSR20190100

58. Robin F, Angenard G, Cano L et al (2020) Molecular profiling of stroma highlights stratifin as a novel biomarker of poor prognosis in pancreatic ductal adenocarcinoma. Br J Cancer 123:72–80. https://doi.org/10.1038/s41416-020-0863-1

Tables

Table 1. Multivariate Cox regression results of prognosis-related PAGs in HCC

| Gene id	Coefficient	HR	HR.95L	HR.95H	P value
SFN	0.116124	1.123135	1.029512	1.225273	0.008925
PRKAA2	0.204509	1.226922	1.011449	1.488299	0.037941
PITX2	0.443949	1.558850	1.049609	2.315162	0.027815
CDK1	0.222894	1.249688	1.043175	1.497084	0.015579

Note: PAGs: the phosphoinositide 3-kinase (PI3K)/protein kinase B (AKT) associated genes; HCC, hepatocellular carcinoma; HR, hazard ratio.

Figures
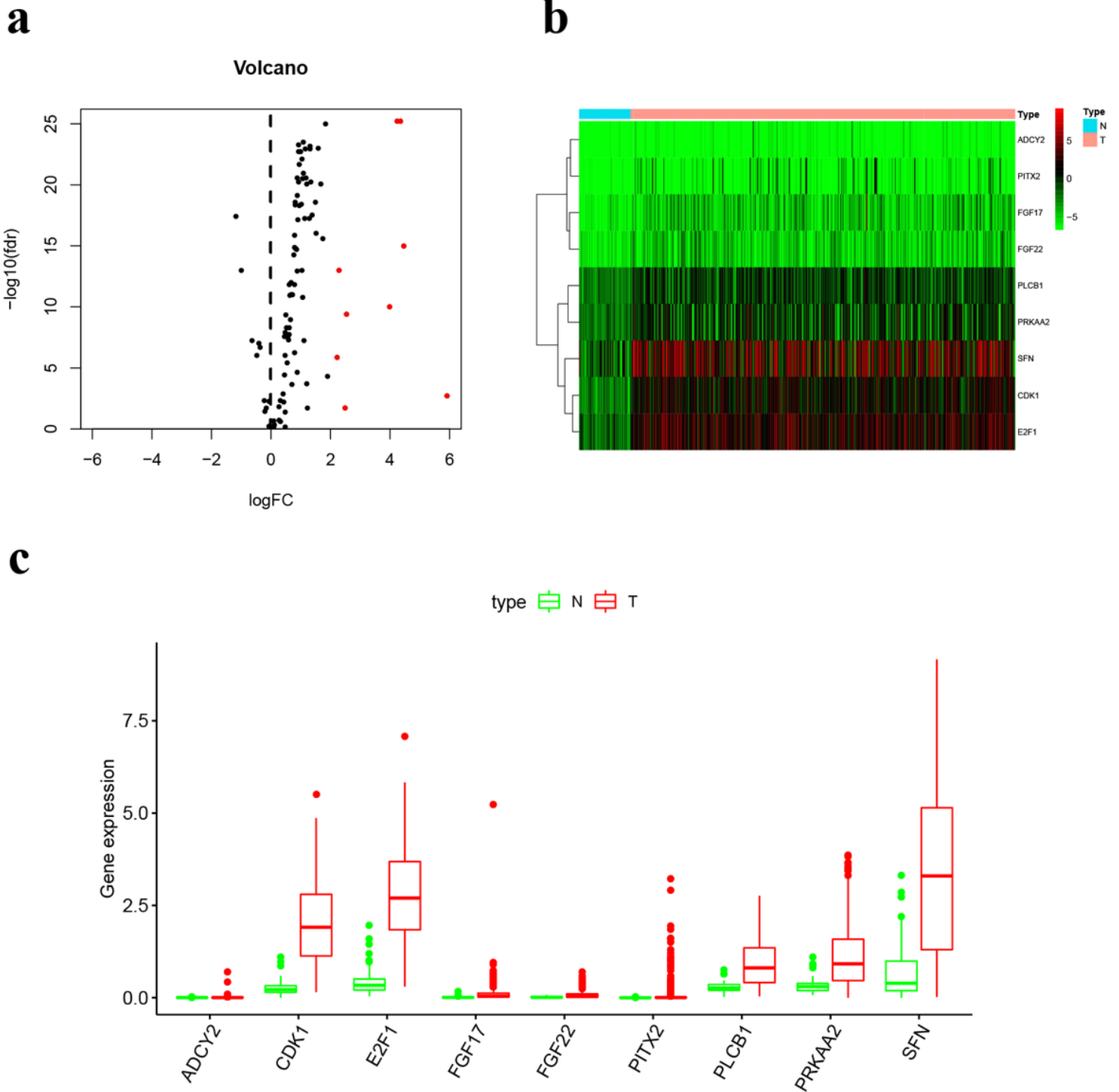
Figure 1

Differentially expressed PI3K/AKT signaling pathway-associated genes (PAGs) between 50 nontumor samples and 374 hepatocellular carcinoma (HCC) samples. (a) The volcano map of 9 upregulated PAGs between the tumor tissue samples and normal tissue samples. Red represented the 9 upregulated PAGs. (b) The heatmap of the 9 upregulated PAGs expression. (c) The boxplot of 9 upregulated PAGs expression.
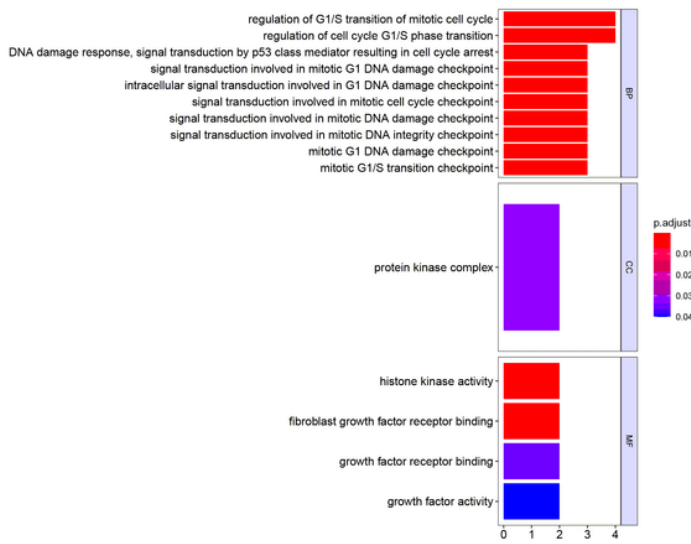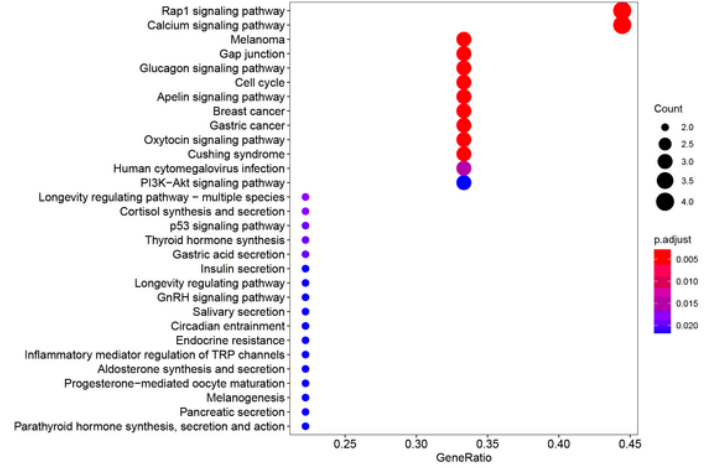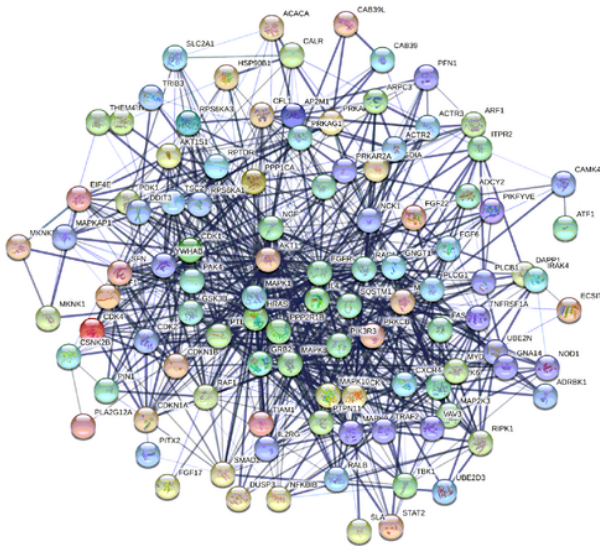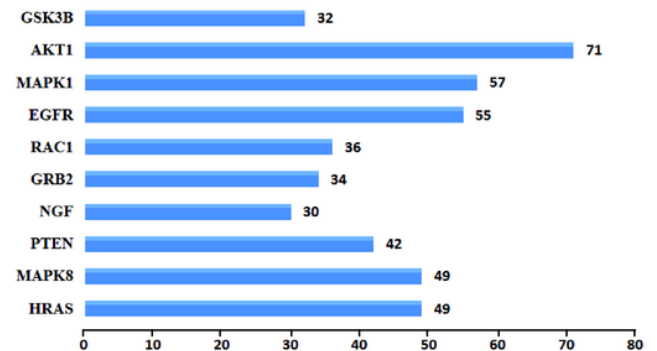
Figure 2

(a) Bar plot of the enriched biological processes, cellular component, and molecular functions in GO enrichment analysis. (b) The KEGG enrichment analysis shows significantly enriched pathways of 9 upregulated PAGs. The node color changes gradually from red to blue in descending order according to the adjusted p-values. The size of the node represents the number of counts. (c) The interaction network of the 105 PAGs in PPI network. (d) The 10 hub genes whose degree of protein interaction was larger than 30 in PPI network.
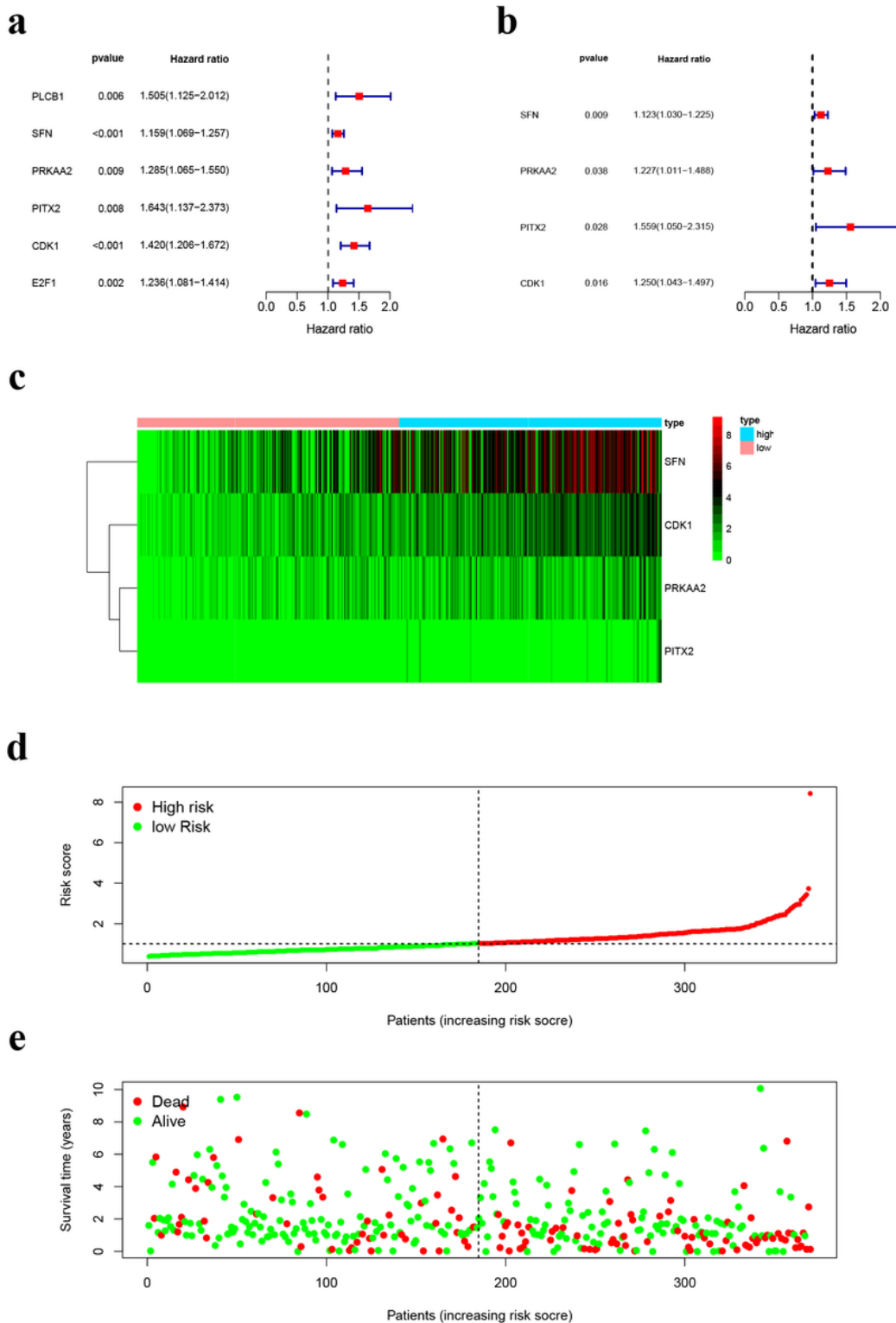
Figure 3

Identification of prognosis related PAGs in HCC. (a) Univariate Cox regression results of prognosis related PAGs in HCC. (b) Multivariate Cox regression results of prognosis related PAGs in HCC. (c) Heatmap of 4 PAGs' expression profile between high and low-risk groups in TCGA database. (d) The risk score distribution of HCC patients in TCGA database. (e) Correlations among the survival times, the survival status and the risk score in TCGA database.
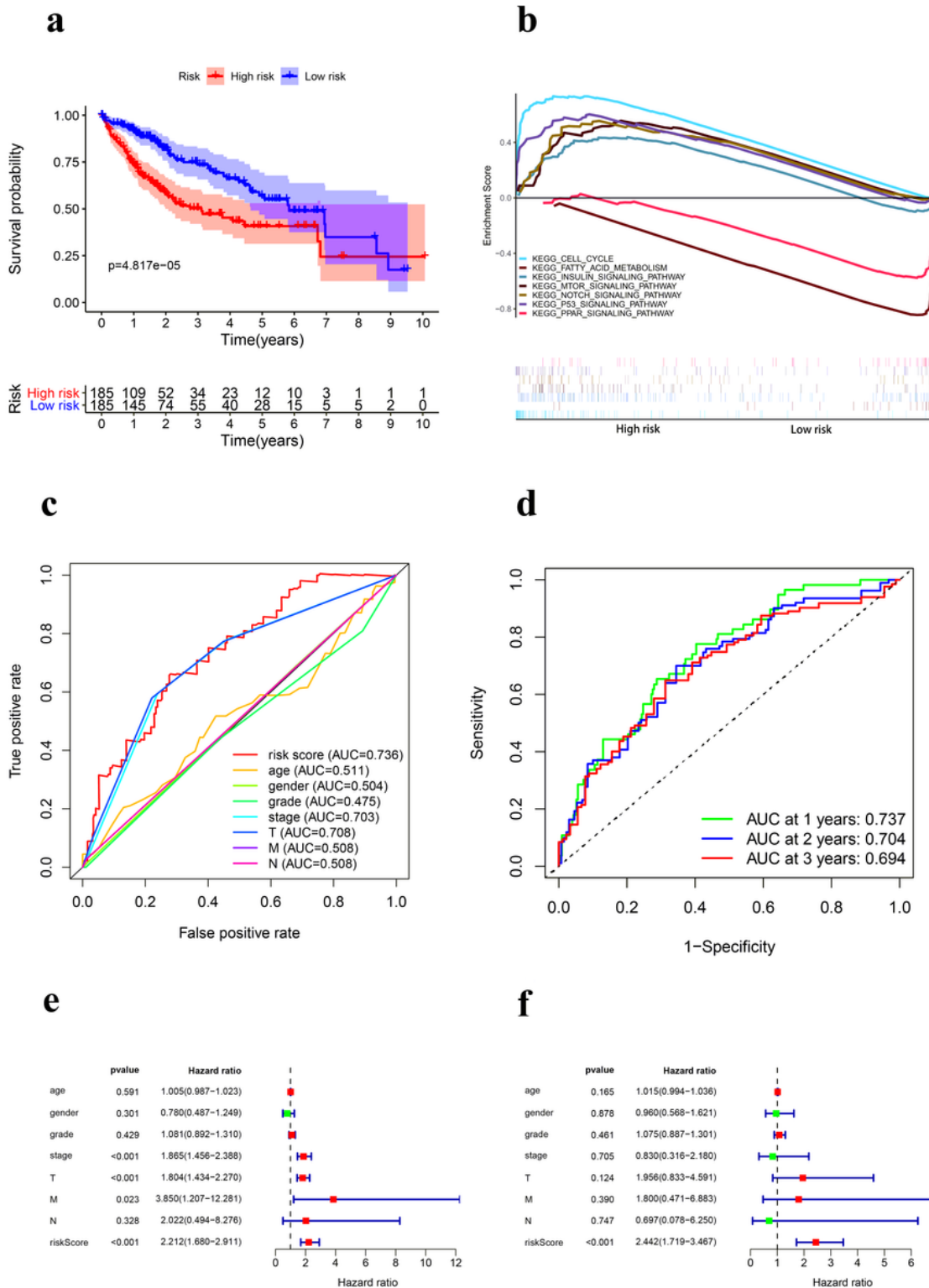
Figure 4

The prognostic value of constructed prognostic signature. (a) Kaplan−Meier (K-M) curve for HCC patients in high/low-risk group in TCGA database. (b) KEGG pathway analysis of the prognostic signature. (c) ROC curve was employed to identify the better prognostic value of risk score compared with other clinicopathological characteristics in HCC. (d) The ROC curve of 1-, 2- and 3- years overall survival in

TCGA database. (e) Univariate Cox regression analysis of risk score in HCC. (f) Multivariate Cox regression analysis of risk score in HCC.
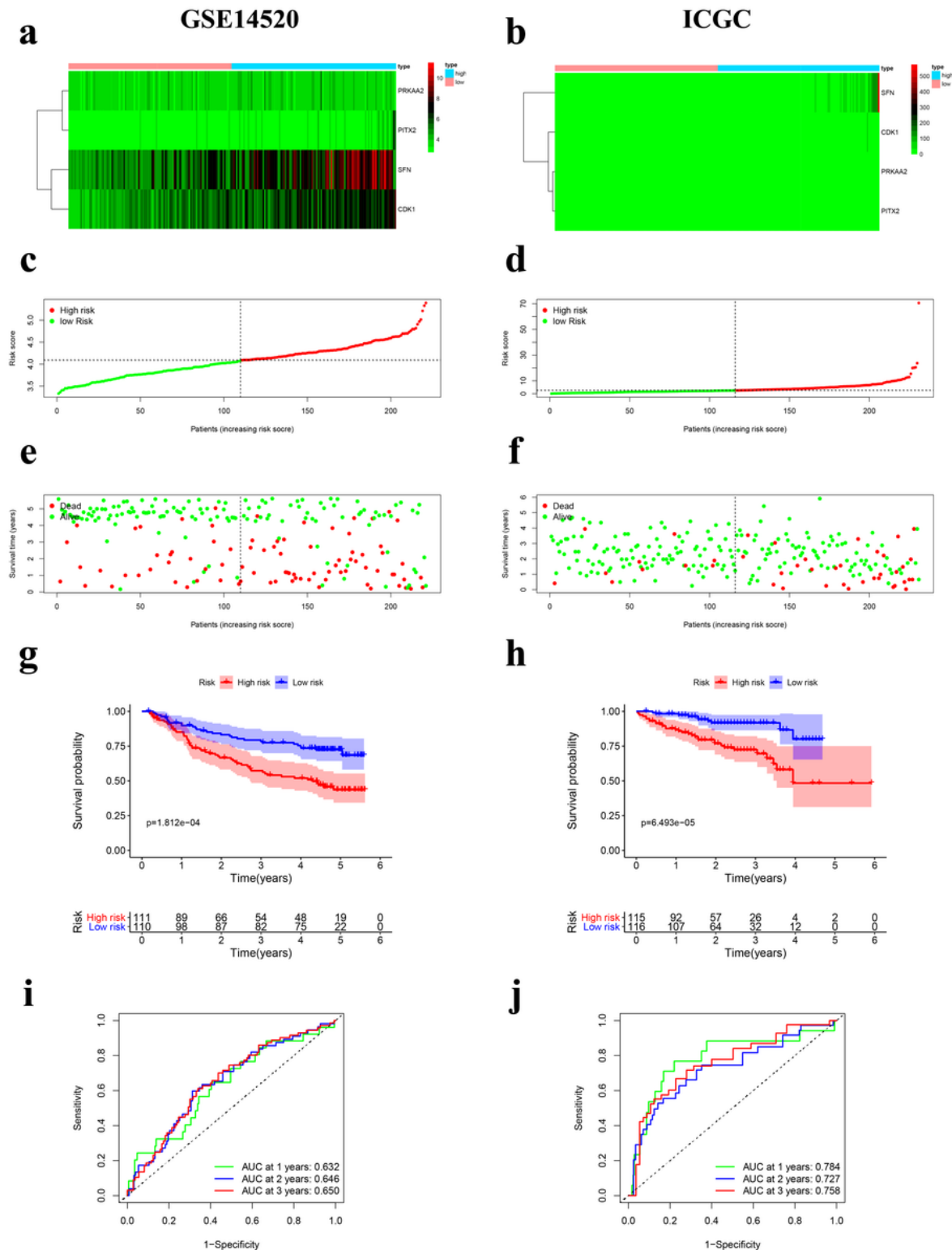
Figure 5

(a) Heatmap of 4 PAGs' expression profile between high and low-risk groups in GSE14520 dataset. (b) Heatmap of 4 PAGs' expression profile between high and low-risk groups in ICGC database. (c) The risk score distribution of HCC patients in GSE14520 dataset. (d) The risk score distribution of HCC patients in

ICGC database. (e) Correlations among the survival times, the survival status and the risk score in GSE14520 dataset. (f) Correlations among the survival times, the survival status and the risk score in ICGC database. (g) Kaplan−Meier (K-M) curve for HCC patients in high/low-risk group in GSE14520 dataset. (h) Kaplan−Meier (K-M) curve for HCC patients in high/low-risk group in ICGC database. (i) The ROC curve of 1-, 2- and 3- years overall survival in GSE14520 dataset. (j) The ROC curve of 1-, 2- and 3- years overall survival in ICGC database.

a
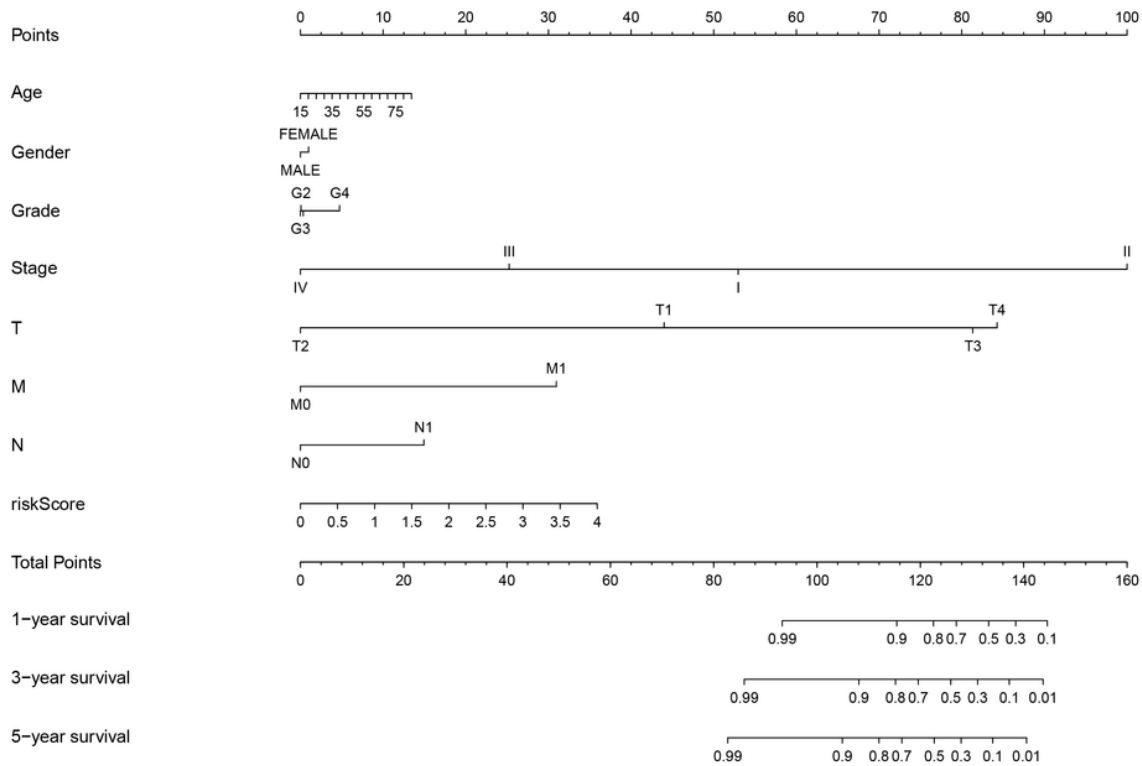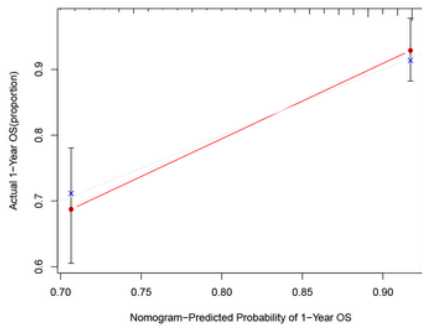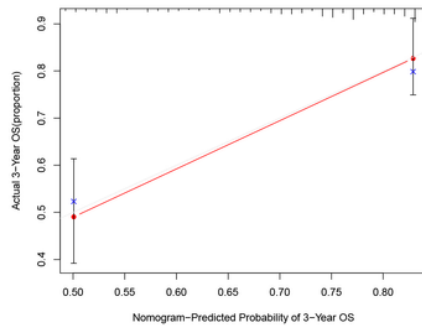
b   c   d
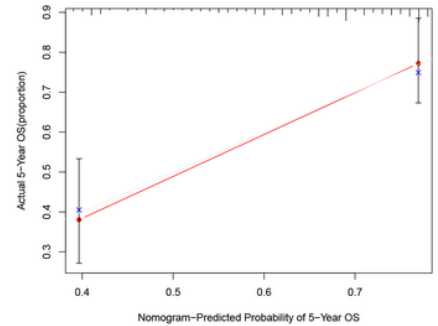
Figure 6

(a) A nomogram predicting the 1-, 3-, and 5- year overall survival of HCC patients. (b) The calibration diagram revealed good coherence between the 1- year overall survival and the prediction of nomogram.

(c) The calibration diagram revealed good coherence between the 3- year overall survival and the prediction of nomogram. (d) The calibration diagram revealed good coherence between the 5- year overall survival and the prediction of nomogram.

a
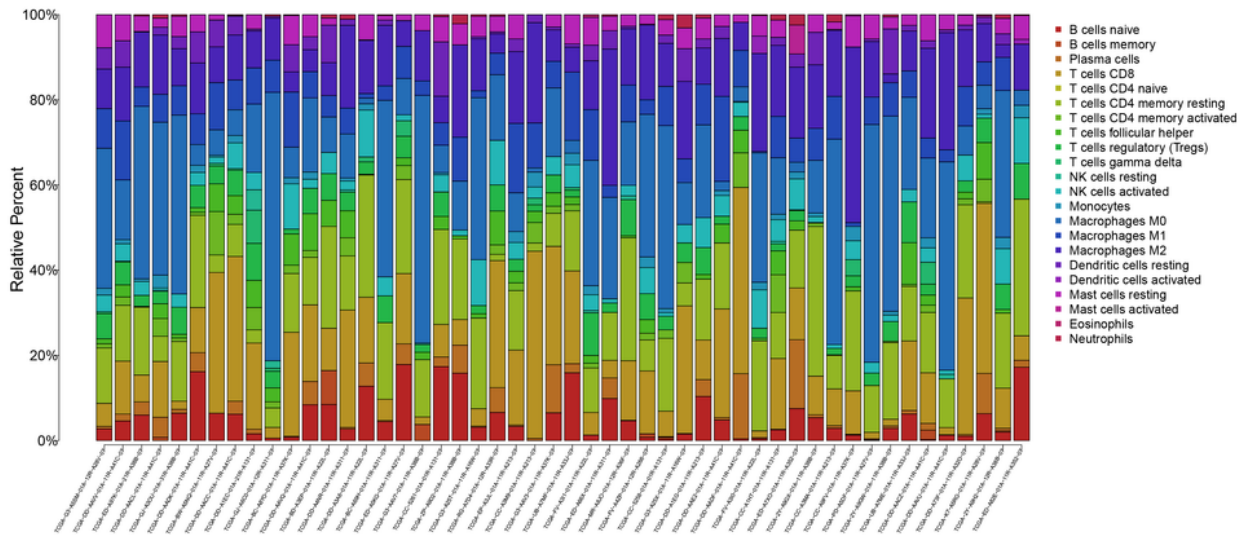
b
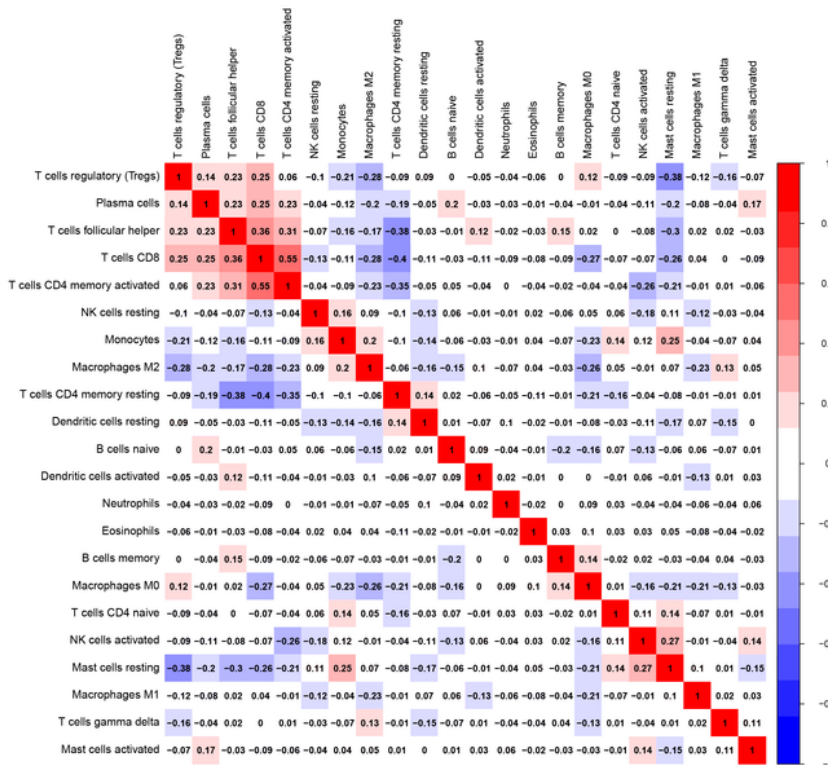
Figure 7

Landscape of tumor infiltrating immune cells in TCGA database. (a) Relative proportion of immune cells in each sample. (b) Relationships of 22 immune cells with each other.
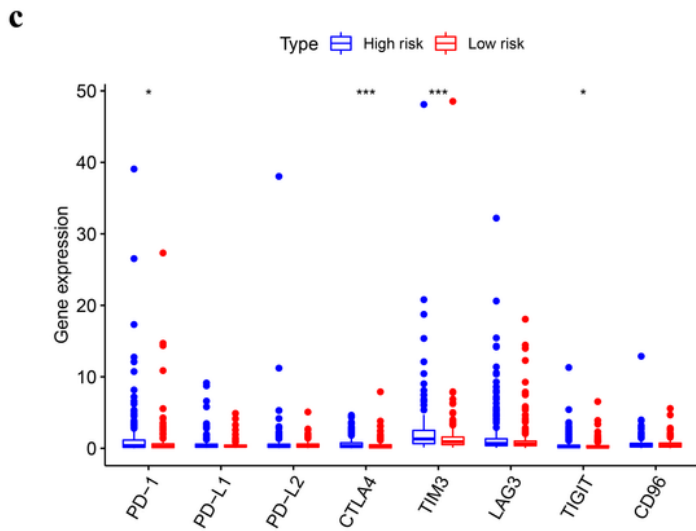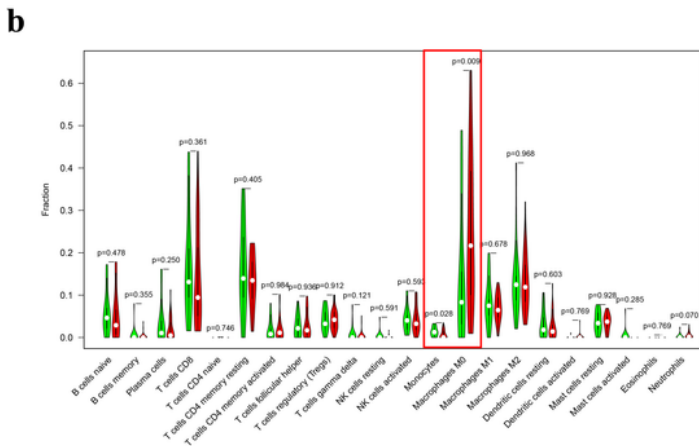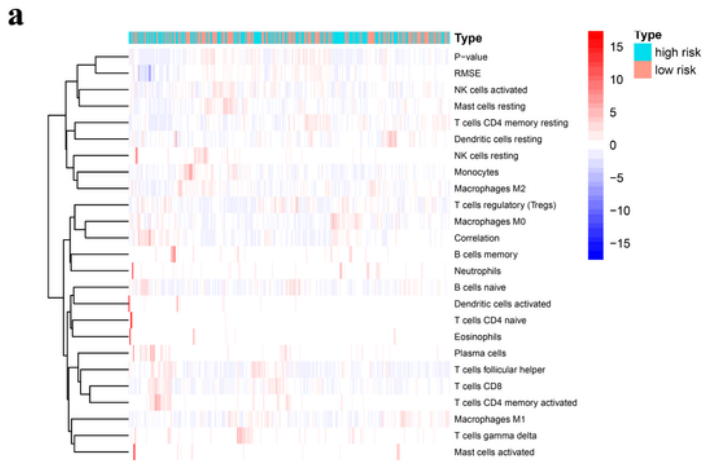
Figure 8

Difference in immune cell infiltration in TCGA database. (a) Heatmap showing the expression profiles of immune cells in different groups. (b) Associations between the risk score and immune cell infiltration. (c) Differential expression of immune checkpoints between low- and high-risk groups in the TCGA database. (*p <0.05, **p <0.01, ***p <0.001).
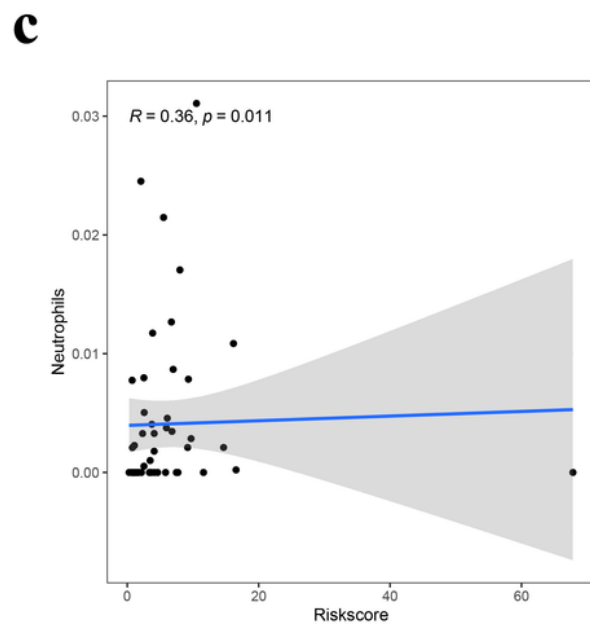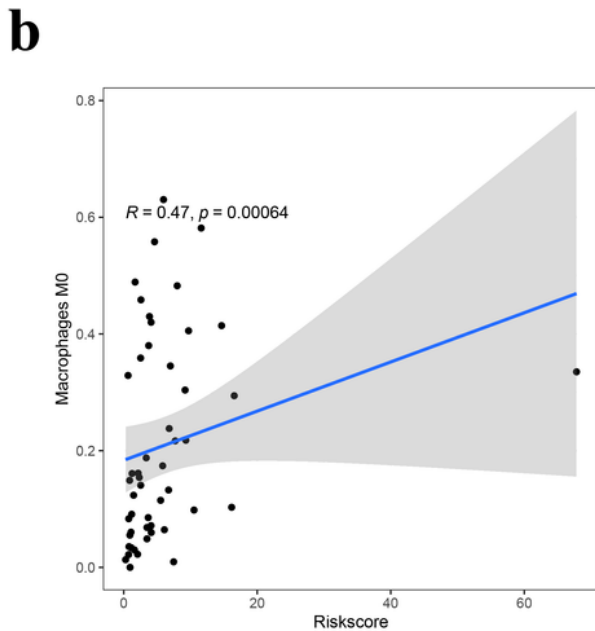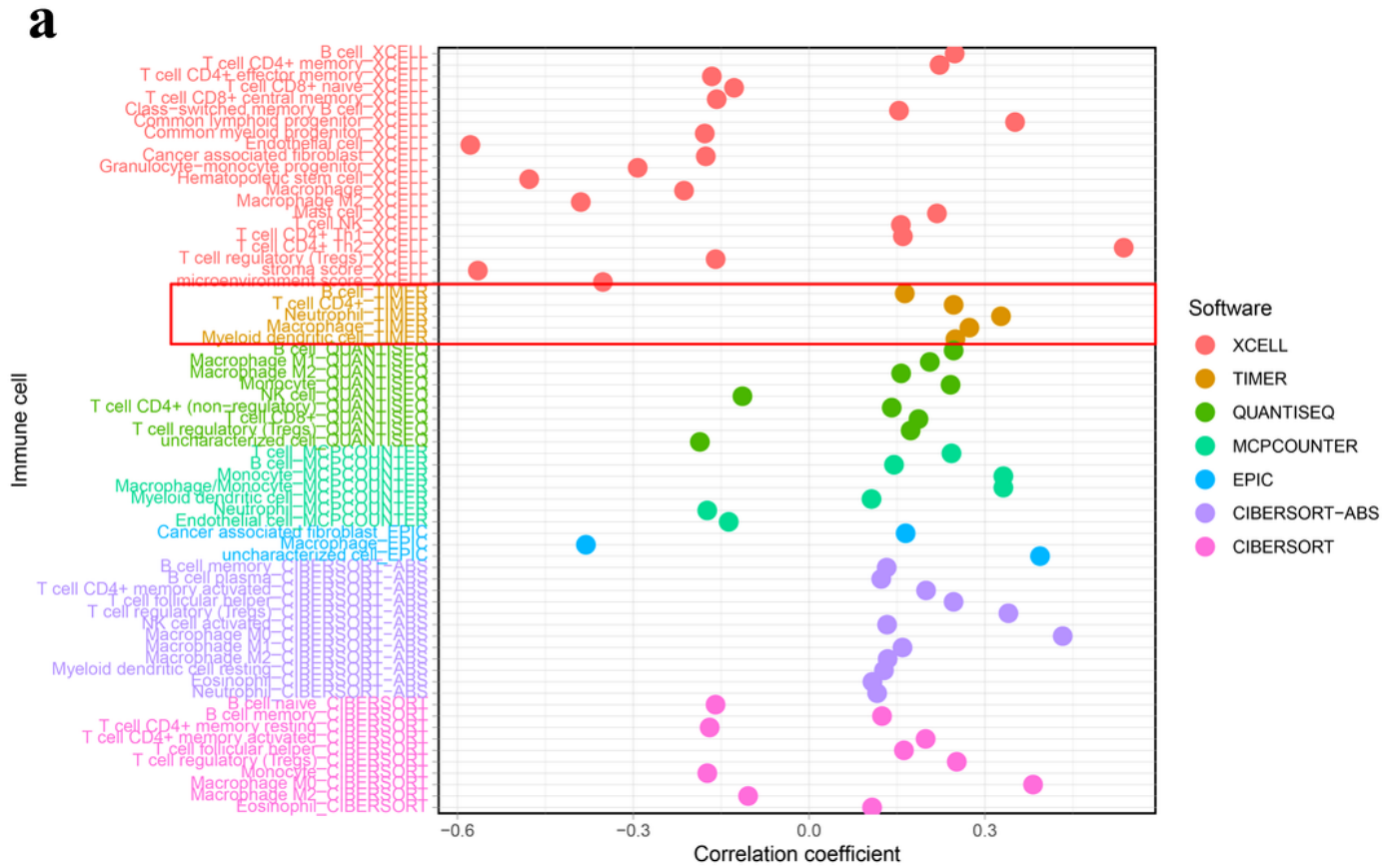
Figure 9

(a) The bubble showed the correlation between the risk score and the infiltrating immune cells in different software. (b) The risk score was positively correlated with the Macrophages M0 and Neutrophils.

Supplementary Files

This is a list of supplementary files associated with this preprint. Click to download.

- Supplementarytable1.docx
- FigureS1.tif
- FigureS2.tif
- FigureS3.tif